Journal of Luminescence 132 (2012) 1705–1713

Contents lists available at SciVerse ScienceDirect

Journal of Luminescence

journal homepage: www.elsevier.com/locate/jlumin

A detailed investigation of the electronic properties of a multi-layer spherical quantum dot with a parabolic confinement

Selçuk Akgül [a], Mehmet Şahin [a,b], Koray Köksal [c,d,*]

[a] Department of Physics, Faculty of Science, Selcuk University, 42075 Konya, Turkey
[b] Department of Material Science and Nanotechnology Engineering, Abdullah Gül University, Kayseri, Turkey
[c] Institut für Physik, Martin-Luther-Universität Halle-Wittenberg, 06120 Halle, Germany
[d] Physics Department, Bitlis Eren University, 13000 Bitlis, Turkey

ARTICLE INFO

Article history:
Received 17 October 2011
Received in revised form
12 January 2012
Accepted 7 February 2012
Available online 15 February 2012

Keywords:
Quantum dot
Intersubband transitions
Electronic structure
Shallow donors
Electron
Confinement

ABSTRACT

In this work, we aim a detailed investigation of the electronic properties of a spherical multi-layer quantum dot with and without a hydrogenic impurity. The structure is introduced in the form of core/shell/well/shell layers. The core and well layers are defined by the parabolic electronic potentials. We carry out the effect of the core radius and layer thickness on the energy levels, their wave functions, binding energies of the impurity and the probability distributions. In order to determine the sublevel eigenvalues and eigenfunctions, the Schrödinger equation is solved full numerically by shooting method in the frame of the effective mass approximation. The results are analyzed in detail as a function of the layer thicknesses and their probable physical reasons are tried to be explained. It is found that the electronic properties and impurity binding energies are strongly depending on the layer thicknesses.

1. Introduction

The technological advances make possible the growth of the perfect two-, one- and zero-dimensional nanosize crystals [1,2]. From the experimental and theoretical works, it is observed that the low-dimensional structures which have amazing optical and electronic properties are very successful candidates for technological applications [3–10]. Particularly, the semiconductors have played very important role in low-dimensional structure technology because they are transition materials between metals and insulators.

The zero-dimensional (0D) structures, in another word quantum dots (QDs), have also great interest because of their unique magnetic, optic and electronic properties. Technologically, the growth of the spherical semiconductor QD structures is possible by using suitable growth techniques [11,12]. Because of their geometrical similarity to the single atom the spherical QDs are named as artificial atom. The semiconductor QDs can be designed in different forms. Today, the most popular example of these forms is multi-layer structures. The production of the multi-layered spherical quantum dot (QD) nanocrystals has been possible since the beginning of the wet chemical synthesis techniques [13–15].

A hydrogenic impurity problem is the most useful model in order to understand many of the electronic and optical properties of an electron in low-dimensional structures for device applications. Pioneering work on the study of the binding energy of a hydrogenic impurity within an infinite potential-well structure has been reported by Bastard [16]. Later, many theoretical and experimental studies have been performed on the properties of impurity states in the quantum well, quantum wire and quantum dot [17,18].

Recently, the electronic properties of multilayered spherical quantum dot under some different physical effects are investigated by some works [19–22]. These studies are related to electronic energy level and impurity binding energy calculations for ground states of a spherical square well. It is seen from these studies the impurity binding energies are very sensitive to the layer thickness.

In this study, we introduce a core/shell/well/shell QD heterostructure with parabolic confinement of the core and well layers. The main aim of this study is to investigate a detail electronic properties of ground and excited states in the core/shell/well/shell spherical QD depending on core radius and layer thicknesses for cases with and without a donor impurity. All results are presented for both cases with ($Z=1$) and without ($Z=0$) the impurity.

* Corresponding author at: Physics Department, Bitlis Eren University, 13000 Bitlis, Turkey. Tel.: +90 434 2285170.
E-mail addresses: sahinm@selcuk.edu.tr (M. Şahin), kkoksal@beu.edu.tr (K. Köksal).

0022-2313/$ - see front matter © 2012 Elsevier B.V. All rights reserved.
doi:10.1016/j.jlumin.2012.02.012

The rest of the paper is organized as follows: in the next section, the model and theory are presented. After that, the results are showed and detailed discussions are given. In the last section, a brief conclusion is presented.

2. The model and theory

In the frame of the effective mass approximation, the Hamiltonian of an electron bound to an on-center donor impurity can be written as

$$H=-\frac{\hbar^2}{2}\nabla_{\mathbf{r}}\left(\frac{1}{m^*(r)}\nabla_{\mathbf{r}}\right)+\frac{\ell(\ell+1)\hbar^2}{2m^*(r)r^2}-\frac{Ze^2}{\varepsilon(r)r}+V(r), \tag{1}$$

where $\hbar$ is reduced planck constant, $m^*(r)$ is the position-dependent effective mass of the electron, r is the radial position of the electron, ℓ is the angular momentum quantum number, $\varepsilon(r)$ is the position-dependent static dielectric constant of the quantum dot and Z is charge of the impurity. In Eq. (1), while the first term on the right-hand-side refers to the kinetic energy of the electron, second term is contribution of the angular momentum to the energy and the third term indicates the attractive Coulomb interaction between the electron and the impurity. It should be noted that while $Z=0$ corresponds to a case without the impurity (i.e. a single electron problem), $Z=1$ corresponds to a case with the impurity. The last term is the radial confinement potential which has a form of

$$V(r)=\begin{cases}\dfrac{V_0}{R_1^2}r^2, & 0<r<R_1;\\ V_0, & R_1<r<R_2 \quad \text{and} \quad r>R_3;\\ \dfrac{V_0}{(R_2-a)^2}(r-a)^2, & R_2<r<R_3.\end{cases} \tag{2}$$

where $a=(R_2+R_3)/2$. The general shape of the quantum dot–quantum well structure and its potential profile can be seen in Fig. 1. The single particle energy levels and wave functions can be found from the solution of Eq. (1) by using shooting method. As well known, this method is used to convert an eigenvalue problem to an initial value problem. For this, the Hamiltonian operator has been discretized on a uniform radial mesh in 1D using the finite differences and Eq. (1) has been reduced to an initial value equation by means of

$$R_{n,\ell}(i+1)=\left(\frac{r}{r+h}\right)\left[2+\frac{2m^*h^2}{\hbar^2}\left(V(i)+\frac{\ell(\ell+1)\hbar^2}{2m^*r^2}-E_{n,\ell}-\frac{Ze^2}{\varepsilon r}\right)\right]\times R_{n,\ell}(i)-\left(\frac{r-h}{r+h}\right)R_{n,\ell}(i-1). \tag{3}$$

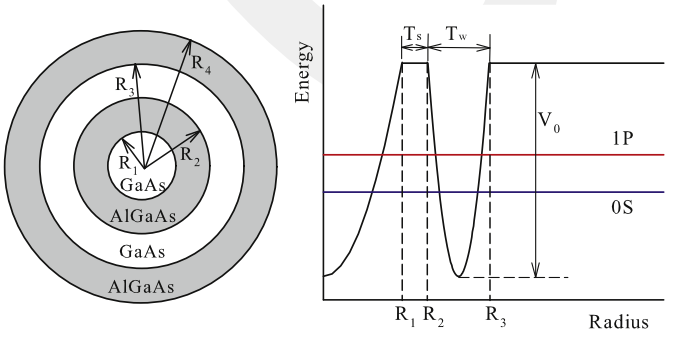

Fig. 1. The schematic representation of a core/shell/well/shell quantum dot and its potential profile in radial direction. While first parabolic shape is used to define the core structure, the second parabolic shape indicates the well structure. T_s and T_w are shell (barrier) and well thicknesses, respectively. Blue and red lines show the 0 s and 1p energy levels. (For interpretation of the references to color in this figure legend, the reader is referred to the web version of this article.)

where i is the index of mesh points and h is the distance between two mesh points. h is chosen as 0.005. The details can be found in Ref. [2].

Because of the spherical symmetry of the system, the angular part of the electron wavefunction is considered as spherical harmonics. The whole wavefunction can be written as

$$\psi_{n,\ell,m}(r,\theta,\phi)=R_{n,\ell}(r)Y_{\ell,m}(\theta,\phi), \tag{4}$$

where $R_{n,\ell}$ is the radial part, n,ℓ,m are the principle, angular and magnetic quantum numbers, respectively. It should be noted that we have taken into consideration the lowest two-level which are 0S and 1P. It is well known that the principle and angular quantum numbers $n=0$, $\ell=0$ for ground state (0S) and $n=1$, $\ell=1$ for first excited state (1P).

The binding energy of the neutral hydrogenic donor impurity is defined as [18]

$$E_b(D^0)=E_{n,\ell}-E_{n,\ell}(D^0), \tag{5}$$

where $E_{n,\ell}$ and $E_{n,\ell}(D^0)$ are the energies of the electron for the non-impurity and impurity cases, respectively.

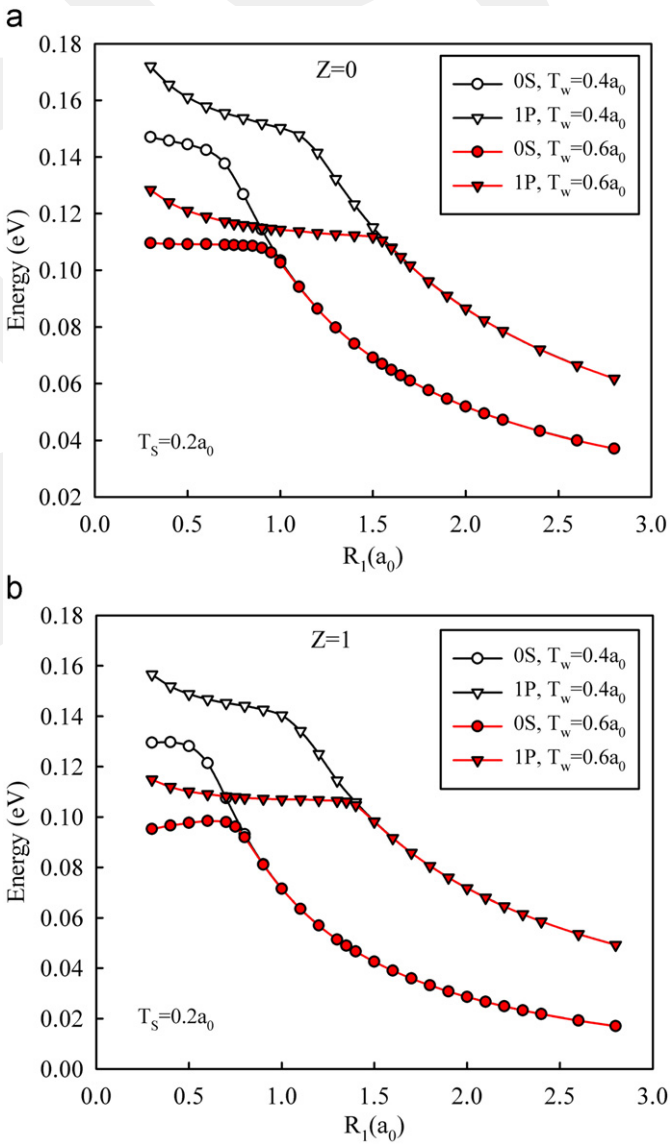

Fig. 2. The variation of the ground and excited state energies as a function of the core radius, R_1, for two different well widths $T_w=R_3-R_2=0.4$, $0.6a_0$ and constant barrier size. The upper and lower figures represent the case of $Z=0$ and $Z=1$, respectively.

3. Results and discussion

In this study, we have chosen GaAs for core and well region and AlGaAs for shell regions in a multi-layer quantum dot (QD) structure. As is well known GaAs have relatively smaller band gap compared to the barrier layers made of AlGaAs. The aluminium content in AlGaAs has been selected in such a way as to avoid strain between the layers. In our calculations, we have used the atomic units where the Planck's constant $\hbar=1$, the electron charge is $e=1$, the bare mass of the electron is $m_0=1$. The effective Bohr radius and Rydberg energy are $1a_0=100$ Å and $1R_y=5.25$ meV. The material parameters have been taken as: $m^*_{GaAs}=0.067m_0$, $m^*_{AlGaAs}=0.088m_0$, $V_0=228$ meV, $\varepsilon_{r(GaAs)}=13.18\varepsilon_0$ and $\varepsilon_{r(AlGaAs)}=12.8\varepsilon_0$.

The energy eigenvalues and corresponding wave functions are obtained by solving Eq. (1) using the electronic potential, Eq. (2). We limit ourselves to consider only the ground (0*S*) and excited states (1*P*) to investigate the electronic properties of the system in the impurity ($Z=1$) and no impurity ($Z=0$) cases. Experimentally, it is also possible to observe *S*–*D* transitions, however, these transitions are weaker due to the small transition probability [23]. Fig. 2 shows the variation of the ground (0*S*) and excited (1*P*) state energies as a function of the core radius in the case of $Z=0$ and $Z=1$, for constant barrier width and two different well sizes. As it can be seen from Fig. 2, all the energy curves show a downward trend with increasing of the core radius, R_1. In both $Z=0$ and $Z=1$ cases, the ground and excited state energies have different values for the small core radius. Because the increase in the core radius reduces the effect of the well width on electronic structure, the ground state eigenvalue energy curves are approaching to each other and overlapping for some specific values of R_1. For excited state energies a similar situation is observed. The physics behind of these observations can be explained as follows. For small R_1 values in 0*S* and 1*P* states, the probability of finding an electron is maximum in the well region as seen from Fig. 3(a). In other words, the 0*S* and 1*P* state electrons are totally confined in the narrow well region and corresponding eigenvalues have the maximum values due to the strong confinement. Therefore, the magnitude of the energy is strongly dependent on the core radius and the well width (inversely proportional to the square of the radius and the width). The increase in the well width causes the decrease in the energy.

As seen from Fig. 2, the ground state energy curves begin to overlap in larger R_1 values ($R_1\approx1.0a_0$ in 0*S* state; $R_1\approx1.5a_0$ in 1*P* state) compared with the case of impurity curves ($R_1\approx0.8a_0$ for 0*S*;$R_1\approx1.4a_0$ for 1*P*). This situation shows that the probability of finding an electron in the core region is increasing with the core radius as seen in Fig. 3(b). If the core radius take a sufficiently large value, the effect of the well size disappears and core/barrier/well/barrier structure can be considered as a simple core/barrier. This situation can be observed easily from Fig. 3(c). In the impurity case, the attractive Coulomb effect of the impurity leads to maximization the probability density in the core region for

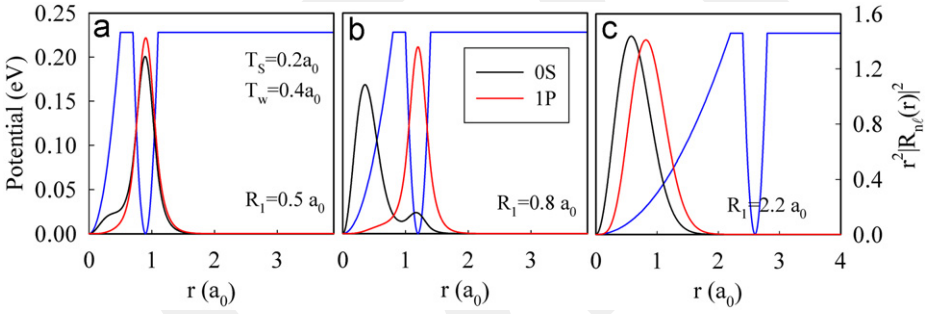

Fig. 3. In the non-impurity case ($Z=0$), the probability distribution of the ground and first excited states versus r (a) $R_1=0.5a_0$, (b) $R_1=0.8a_0$, (c) $R_1=2.2a_0$.

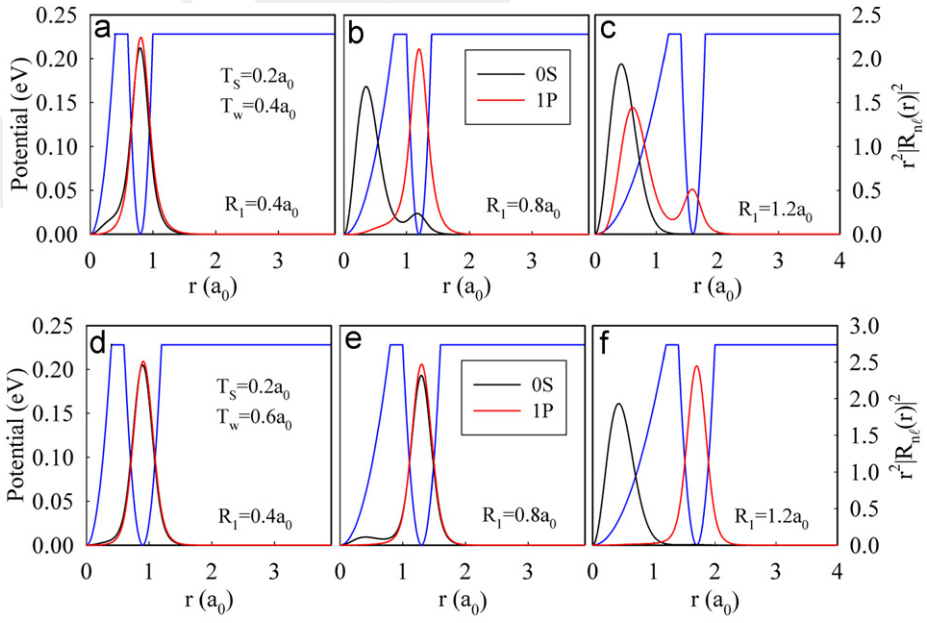

Fig. 4. In the no impurity case ($Z=0$) the probability distribution of the ground and first excited states versus r for $T_w=0.4a_0$ (top panel) and for $T_w=0.6a_0$ (bottom panel).

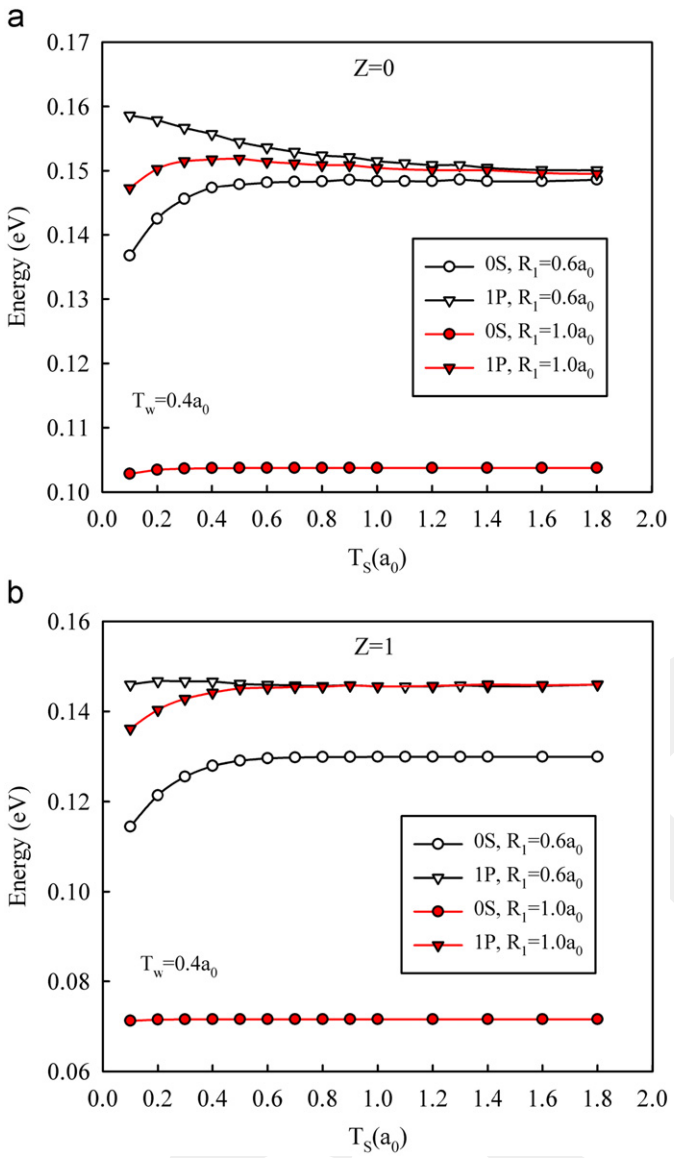

Fig. 5. The ground and excited state energies as a function of barrier size, T_s, for different core radii. Upper and lower figures show the cases of $Z=0$ and $Z=1$.

smaller R_1 values compared to the non-impurity case. Furthermore, this attractive Coulomb potential causes that the energy values in the case of $Z=1$ are lower than those in the case of $Z=0$. Because the attractive Coulomb potential of the impurity is more effective on the ground states than on the higher states, the ground state energy in the case of $Z=1$ is pulled down, the difference between ground and excited state energies is larger than that in the case of $Z=0$.

Fig. 4 shows the probability distribution of the ground and excited states with respect to the radial position, r, in QD for different core radius in the case of $Z=0$. In Fig. 4(a) and (d), $R_1=0.4a_0$ and the occupation probability of the ground and excited states in the well region is maximum. In Fig. 4(b), R_1 is $0.8a_0$ and the maximum point of the ground state occupation probability is shifting to the core region because the core radius is larger than the well width. In Fig. 4(e), the situation is not so different from that of 4(d). In Fig. 4(c) and (f), $R_1=1.2a_0$, because the size of the core region is much larger than that of the well region, the maximum point of the ground state occupation probability is observed in the core region. However, because the well region of QD system in Fig. 4(f) is larger than that of the system in Fig. 4(c), the maximum point of the excited state probability function in Fig. 4(f) and (c) is found in the well region and core region, respectively.

The electronic properties of a multi-layer quantum dot can also be investigated by changing the size of the barrier layer for different specific well and core values. Fig. 5 shows the change of ground and first excited state electron energies as a function of the barrier size in the case of $Z=0$ and $Z=1$, for two different core radius and the constant well width. As can be seen from Fig. 5, in both cases of $Z=0$ and $Z=1$, the curves of the electron energies vary with the increasing of barrier size. After a certain value, the electron energies do not change taking a constant value. The reason of this behavior is that the possibility of tunneling between core and well regions decreases with increasing of the barrier size so that after a certain value of the barrier size the tunneling is not observed at all. It can also be concluded that the ground and excited energy states are affected by only small barrier size.

In Fig. 5, only excited state energies are approaching to each other with increasing barrier size for different core radii in the case of $Z=0$ and $Z=1$. The excited state energy curves begin to overlap in the case of $Z=0$ for $T_s > 1.4a_0$ and in the case of $Z=1$ for $T_s > 0.6a_0$. This situation can be explained as follows: in both

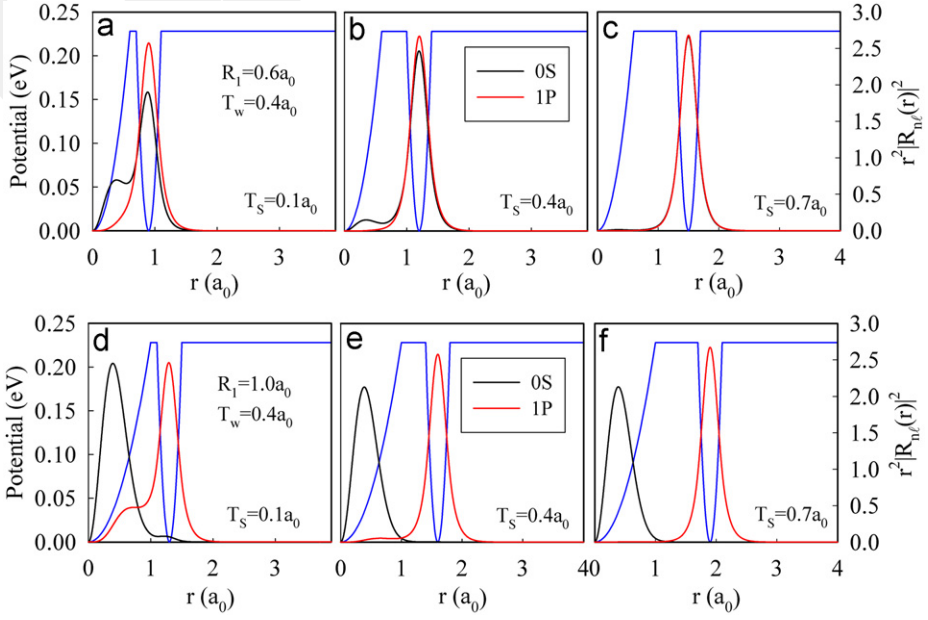

Fig. 6. In the no impurity case ($Z=0$) the probability distribution of the ground and first excited states versus r for $R_1=0.6a_0$ (top panel) and for $R_1=1.0a_0$ (bottom panel).

cases of $Z=0$ and $Z=1$, the occupation probability of an excited state electron increases in the well region and decreases in the core region with increasing barrier size. After a specific barrier size, the core size loses its effect on the system and becomes insignificant. In this point, the system can be considered as a quantum well system. As can be seen from Fig. 5, the energy difference between ground and excited states in the case of $Z=0$ is larger than that in the case of $Z=1$. This is a result of the attractive Coulomb potential of the impurity. In Fig. 5(a), when the core radius is $R_1=0.6a_0$, the difference between ground and excited state energies in the case of $Z=0$ is around 22 meV for small barrier size. This difference is decreasing with increasing barrier size and it becomes 0.9 meV around $T_s=1.8a_0$. This situation can be explained as follows: in the case of $Z=0$ for $R_1=0.6a_0$, the possibility of electron tunneling into the core region decreases with the barrier size. Therefore, the occupation probability of the electron decreases in the core region and increases in the well region. For $R_1=1.0a_0$ in both cases $Z=0$ and $Z=1$, the ground state energy becomes minimum at the smallest value of the core radius. This behavior can be explained by the relationship between the core size and the energy eigenvalues. Because the eigenvalues are inversely proportional to the core radius, the energy increases with shrinkage and decreases with the enlargement of the core width. Therefore, the ground state electron has a small energy value in the case of $Z=0$ and $Z=1$ for $R_1=1.0a_0$, which is the reason of an increase in the occupation probability in the core region.

In order to make more clear the phenomena mentioned in previous paragraph, we can look at the variation of the probability density with the shell thickness. Fig. 6 shows the ground and excited state probability density function for different barrier width, for two different core radii ($R_1=0.6a_0$ and $R_1=1.0a_0$) and for constant well width ($T_w=0.4a_0$) in the case of $Z=0$ and $Z=1$. In Fig. 6(a) and (d), the probability density as a function of core radius can be seen for same well widths and shell thicknesses. Because the core radius in Fig. 6(a) is smaller than those in bottom figures, the ground state electron can make tunneling into the core region, as the excited state electron is totally localized in the well region. Because the core region in Fig. 6(d) is wider than that in Fig. 6(a), the electron energy becomes smaller, the ground state and the excited state probability densities are maximum in the core region and the well region, respectively. The similar comparable situations can be observed between Fig. 6(b)–(e) and (c)–(f).

The well width has a great influence on the electronic properties of the spherical quantum dot structure. In order to investigate well width-dependent electronic properties, we keep the core radius constant for different barrier sizes. In Fig. 7(a) and (b), it can be seen the change of the ground (0*S*) and excited state (1*P*) electron energies for impurity ($Z=1$) and no impurity($Z=0$) cases taking the core radius as $R_1=0.8a_0$ and barrier widths as $T_s=0.2a_0$ and $T_s=0.4a_0$. As known, the energy levels in an isotropic harmonic oscillator potential are in the form of $(2n+\ell+3/2)\hbar\omega$ such that the difference between two energy levels is $\hbar\omega$. The increase in the well size causes lowering of the quantum confinement effect which leads to approaching of two closest energy levels. Therefore, the electrons feel the less confinement effect with the increasing of the well size and the energy levels will take the values of the free particles. According to these explanation, as seen from Fig. 7, in both cases $Z=0$ and $Z=1$, the difference between ground and excited energy levels is maximum when the well width has the smallest value (e.g. $T_w=0.1$ for $T_s=0.2$ and $T_s=0.4a_0$). The energy difference is rapidly decreasing with the rising well width for different barrier size and it is zero after specific values of the well width (the energy difference is zero after $T_w=0.45$ if $T_s=0.2$ and after $T_w=0.7$ if $T_s=0.4$ in the case of $Z=0$, the difference also zero after $T_w=0.65$ if $T_s=0.2$ and after $T_w=0.85$ if $T_s=0.4$ in the case of $Z=1$). In Fig. 7, it can be recognized that the ground and excited energy states of non-impurity system, $Z=0$, are higher than those of the impurity system, $Z=1$. The reason of this, as we mentioned before, is the attractive Coulomb effect of the impurity.

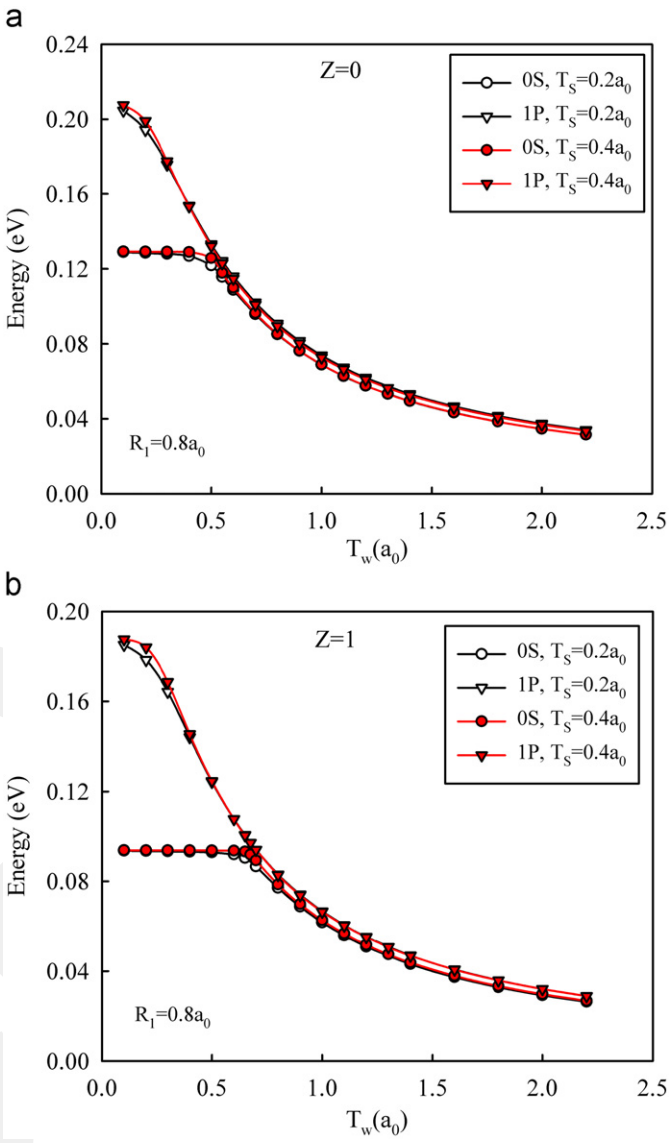

Fig. 7. The ground and excited state energies as a function of the well width, T_w, for different barrier size and constant core radius. Upper and lower figures show the cases of $Z=0$ and $Z=1$.

Fig. 8 shows the probability distribution of the ground and excited states versus increasing well width. In Fig. 8(a)–(c), the size of the barrier and core are taken as constant and the well width is changed. In Fig. 8(a), because the well is very narrow, the ground state probability density has the maximum value in the core region, while the excited state probability density has two maximum peaks in both well and core region. In Fig. 8(a), with the increasing of the well width, the probability density of the 0*S* and 1*P* states starts to be localized in the well region. Same situations are valid in Fig. 8(b) and(c).

Fig. 9 shows the change of the electron energy with the variation of the well width in the case of $Z=0$ and $Z=1$, for constant barrier size ($T_s=0.4a_0$), two different core radius ($R_1=0.4a_0$ and $R_1=0.8a_0$). As it can be seen from Fig. 9(a) and (b), the change

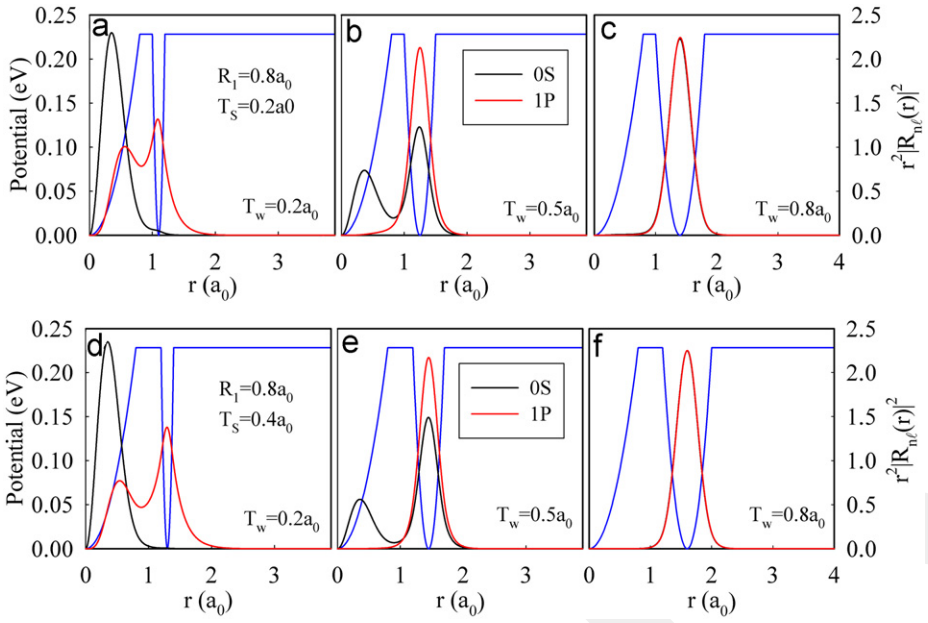

Fig. 8. In the non-impurity case ($Z=0$) the probability distribution of the ground and first excited states versus r for $T_s=0.2a_0$ (top panel) and for $T_s=0.4a_0$ (bottom panel).

in the ground and excited state energies is decreasing with the well width in both cases of $Z=0$ and $Z=1$ for $R_1=0.4a_0$. Furthermore, the difference between ground and excited energy states is extremely small which is caused by the localization of the electron in the well region due to the narrow size of the core region. This situation can be seen also from Fig. 10. The ground state energies remain constant up to the value of $T_w=0.4$ for $Z=0$ and $T_w=0.6$ for $Z=1$ if $R_1=0.8$. The excited state energies for both cases $Z=0$ and $Z=1$ are always decreasing with the increasing of well width. These different trends between the states cause a rapid decrease in the differences of the state energies.

Fig. 10 shows the probability distribution function of the ground and excited electron states with respect to the well size for $Z=0$ case, constant barrier size and two different core radius. In Fig. 10(a), the ground state electron can make tunneling between core and well region of the structure, while the excited state electron is totally localized in the well region. In Fig. 10(d), the excited state electron is tunneling between the regions, while the ground state electron is localized in the core region. These two figures show the effect of the core radius on the probability density. In Fig. 10(c) and (f), the probability distribution of the ground and excited states are maximum in the well region due to the sufficiently large well size.

Fig. 11 shows the variation of the binding energy of the ground and excited energy states with the change of the core radius for constant barrier and well size. In Fig. 11, the ground state binding energy is decreasing up to $R_1=0.6a_0$, then it is increasing sharply up to $R_1=1.1a_0$ and decreasing slowly with further increase of core radius. A similar behavior can be seen for $1P$ state. The binding energy of $1P$ state is decreasing up to $R_1=1.3a_0$, rapidly increasing up to $R_1=1.6a_0$ and slowly decreasing after this R_1 value. The physics behind of this behavior can be explained as follows: the electron probability density in the well region is high if the core radius is very small for both impurity and no impurity cases. The impurity and the increase in core radius have no significant effect on the ground state electron energy in the case of $Z=1$ for very small core values. But the increase in core radius causes a very strong decrease in the electron energy for no impurity case. Therefore, if $R_1<0.6a_0$ the binding energy is decreasing with increasing of the core radius for small core values. The wider the core radius, the more possible the tunneling into the core region becomes, so the attractive Coulomb effect of the impurity affects the energy values. Because of this, after the value of $R_1=0.7a_0$ the impurity binding energy is rapidly increasing. If $R_1>1.1a_0$, the core region loses its confinement effect on the electron and impurity binding energy rapidly decreases with increasing R_1. A similar behavior can be seen for $1P$ state.

In Fig. 11, the difference between the ground and excited state binding energies is small when $R_1<0.6a_0$. The difference is rapidly increasing when $R_1>0.7a_0$. The reason of this can be explained as follows. When $R_1<0.6a_0$, the both ground and excited state electrons are totally localized in the well region. Furthermore, the impurity is not effective on the electron energy in the small core radius. Therefore, the difference between binding energies becomes small. When $0.7<R_1<1.3$, the occupation probability of the ground state electrons in the core region increases, but the probability of the excited state electrons is still high in the well region as seen in Fig. 12. Therefore, the effect of the impurity is more dominant on the ground state electron energies than on the excited state ones.

Fig. 12 shows the change of the probability distribution of the ground and excited states with respect to the radial position, r, for different core radii, constant well and barrier widths in the case of $Z=0$ and $Z=1$. As seen from Fig. 12(a) and (d), the impurity has no significant effect on the ground and excited state probability distribution. In Fig. 12(b) and (e), the effect of the impurity can be seen easily on the ground state probability density. In Fig. 12(c) and (f), the impurity is effective on the excited state probability density.

Fig. 13 shows the binding energy as a function of the barrier width for constant core radius and well width. The layer parameters of the structure are $R_1=0.4a_0$ and $T_w=0.2a_0$. As seen from Fig. 13, the ground state binding energy is rapidly decreasing up to $T_s=0.8a_0$. And after that, it approaches a constant value, 13 meV. The excited state binding energy is rapidly decreasing up to $T_s=0.6a_0$, then it starts to decrease more slowly. The variation of the binding energies can be explained as follows: when $T_s=0.1a_0$, the occupation probability of the ground state electron is high in the well region and same electron feels the effect of the impurity due to the smallness of the barrier. With the increase in the barrier size, this effect on the electron becomes less and the binding energy begin to decrease. After a critical value of the barrier size, the ground state electron in the well region cannot

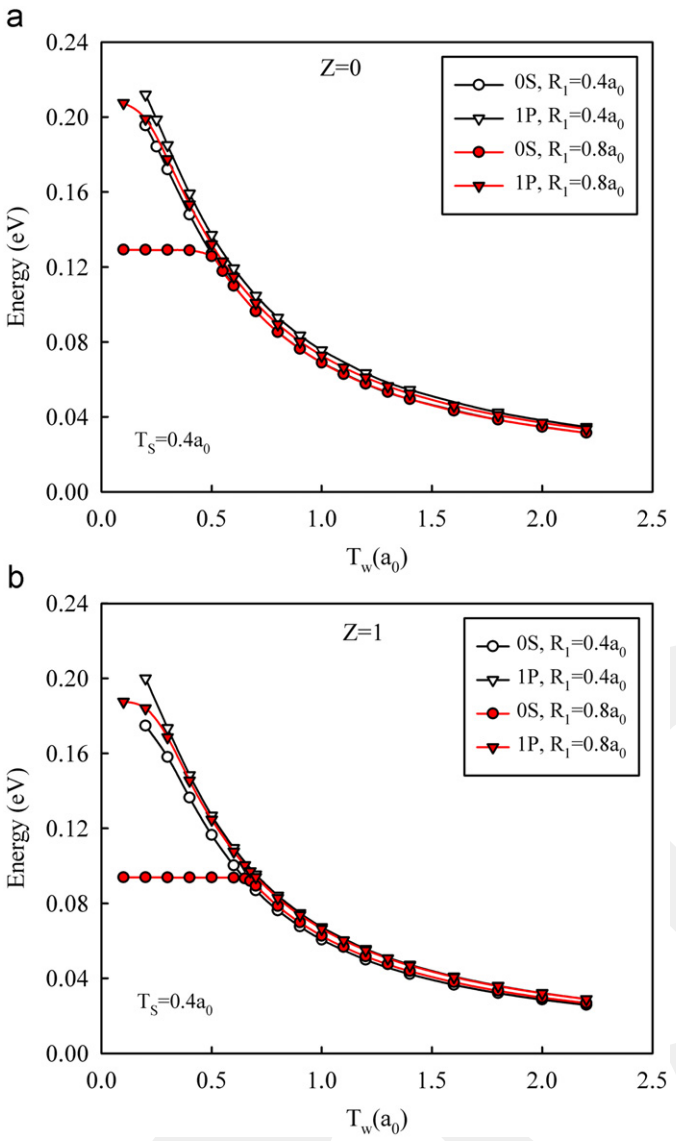

Fig. 9. The change of the energies of ground and excited states with the change of well width for different core radii and constant barrier sizes. Upper and lower figures show $Z=0$ and $Z=1$ cases.

feel the effect of the impurity at all and the ground state binding energy takes a constant value. This situation is very similar to that of the excited state binding energy.

Fig. 14 shows the impurity binding energy as a function of the well width for constant barrier, $T_s=0.4a_0$ and three different core radii. In Fig. 14, the ground and excited state binding energies are decreasing with increase in well width. In Fig. 14(a), when $T_w<0.5a_0$ the ground state impurity binding energy is rapidly decreasing, when $T_w>0.5a_0$ the binding energy is slowly decreasing. The excited state binding energy is decreasing with increase in well width. The ground and excited state binding energies begin to overlap when $T_w>0.6a_0$. As seen in Fig. 14(b), the ground state binding energy curve has a slow decreasing when $T_w<0.2a_0$, the decreasing becomes rapid when $T_w>0.2a_0$ and the curve is approaching to a constant value when $T_w>0.5a_0$. In Fig. 14(c), the ground state binding energy is slowly decreasing with the well size for small well values. The binding energy begins to rapidly decrease between $T_w=0.4$ and $T_w=0.7a_0$ and the decreasing becomes smaller when $T_w>0.7a_0$. In same figure, the excited state binding energy curve has a rapid decreasing trend when $T_w<0.3a_0$, then a slow decreasing when $0.3<T_w<0.7$.

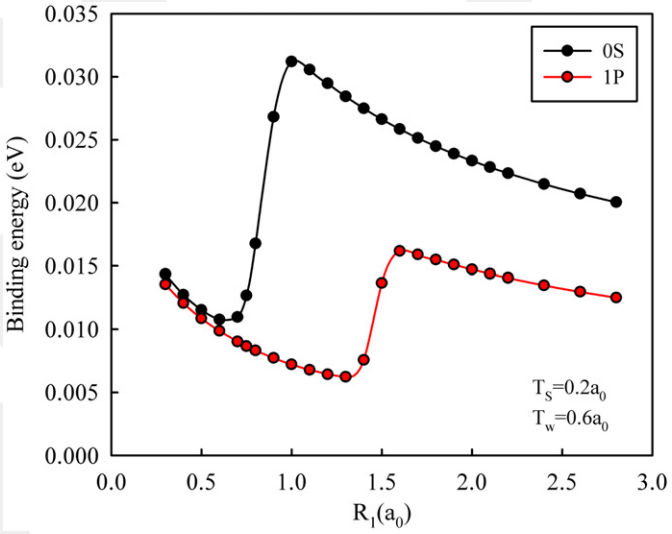

Fig. 11. The change of the binding energies of ground and excited states with the change of core radius.

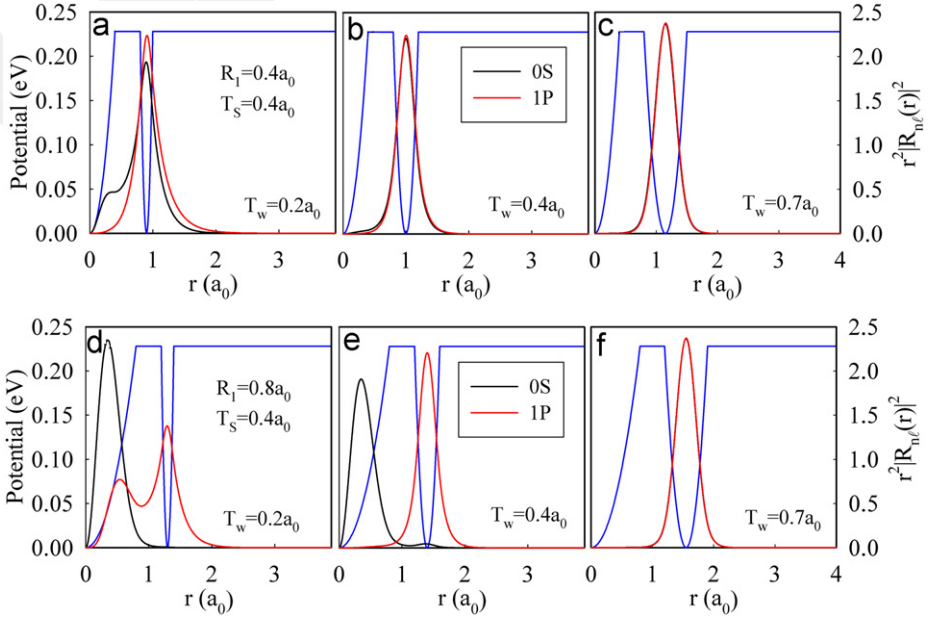

Fig. 10. In the non-impurity case ($Z=0$) the probability distribution of the ground and first excited states versus r for $R_1=0.4a_0$ (top panel) and for $R_1=0.8a_0$ (bottom panel).

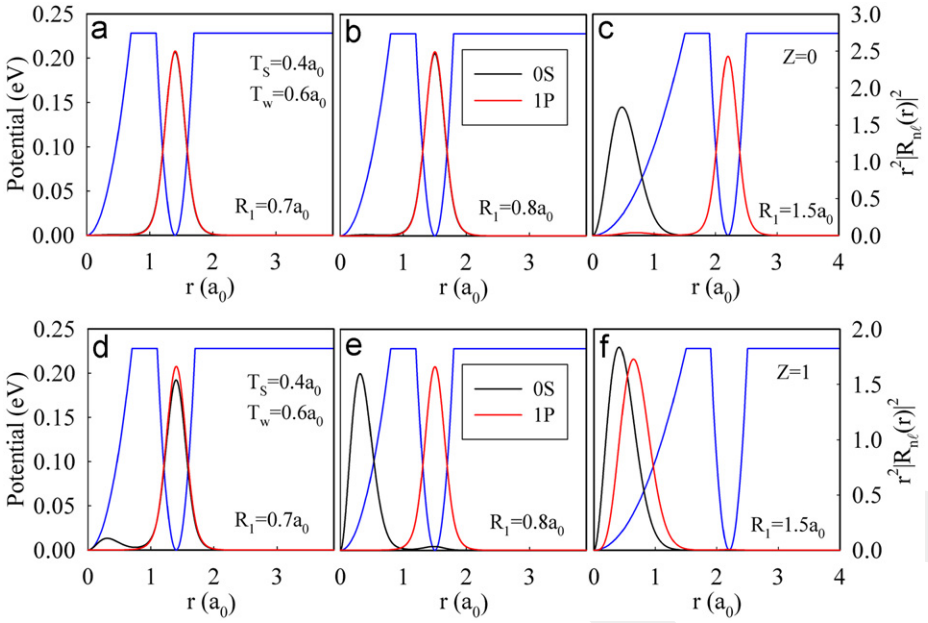

Fig. 12. The probability density function of the ground and excited states with respect to r for constant barrier and well size for no impurity case (top panel) and impurity case (bottom panel).

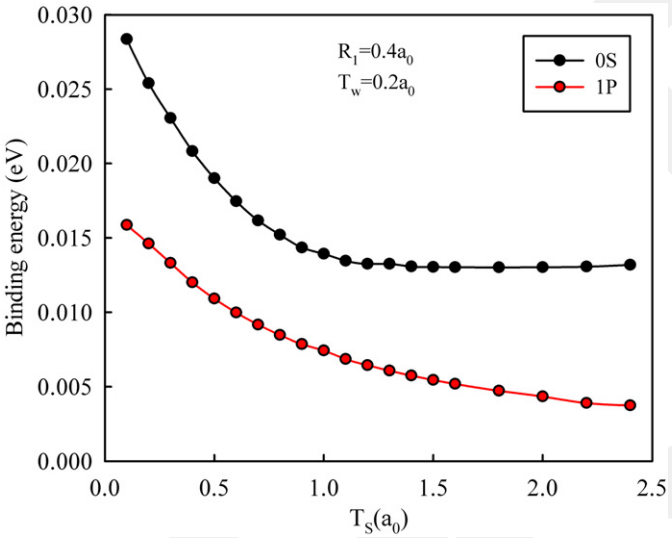

Fig. 13. The change of the binding energies of ground and excited states with the change of barrier width.

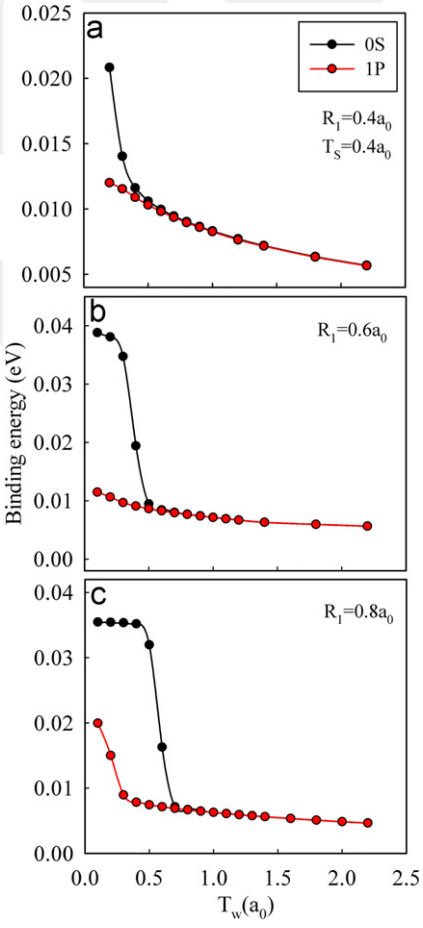

Fig. 14. The change of the binding energies of ground and excited states with the change of well width (a) $R_1=0.4a_0$ (b) $R_1=0.6a_0$ (c) $R_1=0.8a_0$.

If $T_w > 0.7$, the excited state binding energy is approaching to a constant value. This behavior can be explained as follows: when T_w is minimum, the ground state binding energy becomes maximum and the electron occupation probability in core region becomes high. When the well width is increased, the occupation probability of the electron in core region is decreasing so that the impurity loses its effect on the energy. Therefore, the binding energy decreases with the well width. For very large quantum well, the electron behaves as a free electron, the ground and excited state energies approach to the free electron energy values.

4. Conclusion

We have investigated the variation of the electronic structure of the core/shell/well/shell parabolic multi-layer quantum dots by tuning the size of the layers and observed the change of the electronic properties in the presence and absence of a donor impurity. As quantum dot materials, we have used GaAs in core and well layers and AlGaAs in the barrier (shell) layers.

The material parameters have been taken from the literature. The electron eigenvalues and eigenfunctions has been found by using the full numerical shooting technique in the frame of the effective mass approximation. We have compared the systems with and without impurity. We have concluded that the attractive Coulomb effect of the impurity results in significant change of the electronic structure of the multi-layer quantum dot. The size of the barrier, well and core layers are also effective to determine the electronic properties of the system. In this study, we only consider the 0*S* and 1*P* electronic states to investigate. We have showed that the probability densities change for different values of the well, barrier and core sizes. We also have calculated and analyzed the variation of the ground and excited state binding energies with the change of the layer size.

Acknowledgments

This study is a part of M.Sc. thesis which is prepared by S. Akgül. The authors thank Selçuk University BAP Office and TUBITAK for their financial support.

References

[1] D. Bimberg, M. Grundmann, N.N. Ledentsov, Quantum Dot Heterostructures, Wiley, Chichester, 1999.
[2] P. Harrison, Quantum Wells, Wires and Dots: Theoretical and Computational Physics, second ed., John Wiley, New York, USA, 2005.
[3] S. Nizamoglu, T. Erdem, H.V. Demir, Opt. Lett. 36 (2011) 1893.
[4] H. Yildirim, C. Bulutay, Phys. Rev. B 78 (2008) 115307.
[5] C. Bulutay, M. Kulakci, R. Turan, Phys. Rev. B 81 (2010) 125333.
[6] W. Xie, Solid State Commun. 151 (2011) 545.
[7] M. Şahin, Phys. Rev. B 77 (2008) 045317.
[8] M. Şahin, J. Appl. Phys. 106 (2009) 063710.
[9] E.C. Niculescu, Opt. Commun. 284 (2011) 3298.
[10] B. Gönül, E. Bakır, K. Köksal, Semiconductor Sci. Technol. 21 (2006) 876.
[11] X.G. Peng, L. Manna, W.D. Yang, J. Wickham, E. Scher, A. Kadavanich, A.P. Alivisatos, Nature 404 (2000) 59.
[12] H. Weller, A. Eychmüller, Semiconductor Nanoclusters: Physical, Chemical, and Catalytic Aspects (Studies in Surface Science and Catalysis) 103 (1997) 5.
[13] D. Dorfs, A. Eychmüller, Multishell semiconductor nanocrystals, in: A.L. Rogach (Ed.), Semiconductor Nanocrystal Quantum Dots Synthesis, Assembly, Spectroscopy and Applications, Springer-Verlag, Wien, 2008.
[14] D. Dorfs, A. Eychmüller, Nano Lett. 1 (2001) 663.
[15] A. Mews, A. Eychmüller, M. Giersig, D. Schooss, H. Weller, J. Chem. Phys. 82 (1994) 552.
[16] G. Bastard, Phys. Rev. B 24 (1981) 4714.
[17] G.W. Bryant, Phys. Rev. B 31 (1985) 7812.
[18] N. Porras-Montenegro, S.T. Perez-Merchancano, Phys. Rev. B 46 (1992) 9780.
[19] C.Y. Hsieh, D.S. Chuu, J. Phys.: Condens. Matter 12 (2000) 8641.
[20] S. Aktas, F.K. Boz, Physica E 40 (2008) 753.
[21] F.K. Boz, S. Aktas, A. Bilekkaya, S.E. Okan, Appl. Surf. Sci. 255 (2009) 6561.
[22] F.K. Boz, S. Aktas, A. Bilekkaya, S.E. Okan, Appl. Surf. Sci. 256 (2010) 3832.
[23] D. Pan, E. Towe, S. Kennerly, Appl. Phys. Lett. 73 (1998) 1937.